

Review

Characterization and Evaluation of Human–Exoskeleton Interaction Dynamics: A Review

Stefano Massardi ^{1,2}, David Rodriguez-Cianca ¹, David Pinto-Fernandez ^{1,3}, Juan C. Moreno ¹,
Matteo Lancini ⁴ and Diego Torricelli ^{1,*}

¹ Neural Rehabilitation Group, Cajal Institute, Spanish National Research Council (CSIC), 28006 Madrid, Spain; stefano.massardi@cajal.csic.es (S.M.); david.rodriguez.cianca@csic.es (D.R.-C.); david.pinto@cajal.csic.es (D.P.-F.); jc.moreno@csic.es (J.C.M.)

² Department of Mechanical and Industrial Engineering (DIMI), University of Brescia, 25100 Brescia, Italy

³ Universidad Politécnica de Madrid (UPM), 28040 Madrid, Spain

⁴ Department of Medical and Surgical Specialties, Radiological Sciences and Public Health (DSMC), University of Brescia, 25100 Brescia, Italy; matteo.lancini@unibs.it

* Correspondence: diego.torricelli@csic.es

Abstract: Exoskeletons and exosuits have witnessed unprecedented growth in recent years, especially in the medical and industrial sectors. In order to be successfully integrated into the current society, these devices must comply with several commercialization rules and safety standards. Due to their intrinsic coupling with human limbs, one of the main challenges is to test and prove the quality of physical interaction with humans. However, the study of physical human–exoskeleton interactions (pHEI) has been poorly addressed in the literature. Understanding and identifying the technological ways to assess pHEI is necessary for the future acceptance and large-scale use of these devices. The harmonization of these evaluation processes represents a key factor in building a still missing accepted framework to inform human–device contact safety. In this review, we identify, analyze, and discuss the metrics, testing procedures, and measurement devices used to assess pHEI in the last ten years. Furthermore, we discuss the role of pHEI in safety contact evaluation. We found a very heterogeneous panorama in terms of sensors and testing methods, which are still far from considering realistic conditions and use-cases. We identified the main gaps and drawbacks of current approaches, pointing towards a number of promising research directions. This review aspires to help the wearable robotics community find agreements on interaction quality and safety assessment testing procedures.

Keywords: exoskeletons; wearable robots; physical human–exoskeleton interaction; safety; forces; pressures



Citation: Massardi, S.; Rodriguez-Cianca, D.; Pinto-Fernandez, D.; Moreno, J.C.; Lancini, M.; Torricelli, D. Characterization and Evaluation of Human–Exoskeleton Interaction Dynamics: A Review. *Sensors* **2022**, *22*, 3993. <https://doi.org/10.3390/s22113993>

Academic Editor: Carlo Ricciardi

Received: 29 April 2022

Accepted: 23 May 2022

Published: 25 May 2022

Publisher's Note: MDPI stays neutral with regard to jurisdictional claims in published maps and institutional affiliations.



Copyright: © 2022 by the authors. Licensee MDPI, Basel, Switzerland. This article is an open access article distributed under the terms and conditions of the Creative Commons Attribution (CC BY) license (<https://creativecommons.org/licenses/by/4.0/>).

1. Introduction

Exoskeletons are starting to be extensively used in many applications, spanning from military to industrial use, personal care, and medical applications. This is reflected by an increasing trend in the number of devices present on the market [1]. Their range of applicability is expanding together with the evolution of automatized industrial processes—which still require the involvement of human workers [2,3]—and the aging of the population. Aging is associated with increasing mobility impairments, making the demand for rehabilitation and assistive devices grow every year [4]. The use of exoskeletons in rehabilitation medicines represents one of the most grounded scenarios in their future development. Applications such as supporting mobility of spinal cord injured (SCI) persons and rehabilitation of major trauma patients remains the primary focus of exoskeleton research [4].

Due to the increasingly aging population [5], new scenarios are starting to receive attention, not only in the field of after-treatment therapies but also to help elderly people to remain independent by providing daily life assistance [6]. In several of these activities, exoskeletons help users to perform tasks by providing assistance and augmentation of individual capabilities through increasing the range of motion of individual joints [7].

Safety and user acceptability will be the underlying evaluation criteria for the mechanical design, actuation, and control architectures of future exoskeleton developments [5]. One fundamental aspect that differentiates exoskeletons from other robotic technologies is the intrinsic and close physical interaction with humans, defined as the generation and exchange of a net flux of power between both actors [5]. ISO 13482:2014 [6] states how physical interaction (e.g., contact forces) between robot and human will be designed to be as low as reasonably practicable. However, current international standards do not provide realistic protocols to assess contact safety, and in the case of exoskeletons, regulatory gaps are yet to be addressed [7,8].

In exoskeletons, force or torque are usually transferred through attachment devices (i.e., connection cuffs or orthoses) [9] producing interaction forces that are key in the generation of shear stresses, interface movements, and misalignments [10]. This physical interaction between the human user and the wearable robot should be carefully monitored and controlled since an unexpected behavior by one of the actors during the task might have an impact on safety and the system. For this reason, a crucial challenge in exoskeleton design is to minimize the risks introduced by the dynamic interaction between the human and the exoskeleton's physical interfaces. A truly ergonomic physical interface should be customized to an individual's own anthropometrics and needs [11]. However, this concept is unlikely to be applicable to most current devices as they follow a design adaptation concept to fit a large spectrum of possible users. However, how the predefined interface can influence physical human–exoskeleton interaction (pHEI) remains to be defined in a more generalized way. There is still considerable room for the research on pHEI to grow compared with other more accepted fields. Current exoskeleton evaluation processes often include tests with humans for the evaluation of physiological, kinematic, and kinetic effects of human–device interaction [12], but metrics and protocols able to characterize pHEI are still not clarified, preventing standardized pHEI evaluations. Additionally, different metrics can be difficult to apply to a broad spectrum of devices, and the selection of an accepted relevant set of metrics is far from being accomplished. Testbed platforms for proving exoskeleton compliance with contact safety requirements are still limited and developed for specific device solutions [13], while traditional comfort evaluations are based on subjective pain rating scales [14–16]. Qualitative feedback can be improved by user-centered designs and individual needs assessments [17] but do not normally include quantitative measurements able to produce a well-accepted body of scientific knowledge in the field of pHEI. In this growing and partially unexplored field, the necessity to concentrate the future efforts in a common direction is a pressing requirement for the wearable robot community.

The aim of this work is to systematically review recent studies including pHEI measurements such as contact forces, torques, and pressures in order to summarize and analyze the current knowledge, techniques, and metrics used in pHEI measurement. This work answers to the need for building a comprehensive revision of pHEI-related works in an effort to create a first step in the acceptance of a shared set of metrics and methods in pHEI measurement and their safety assessment.

2. Materials and Methods

We define pHEI measurement as any extraction of information related to forces (including torques and pressures) exchanged between a human and an exoskeleton during the execution of a task. Considering the recent and rapid growth of exoskeletons in the last year, we decided not to include studies older than 10 years as they are likely considering depreciated and early-stage devices that are now better equipped and developed. Similar growth is also seen in the world of sensor technologies; for these reasons, various searches were conducted on the Scopus scientific database between 1 January 2010 and 31 December 2021. We looked for articles that included references to human–exoskeleton interaction databases using the AND/OR/NOT Boolean operators with different combinations of terms from 3 sets of keywords:

- exoskeleton*, physical assist*, wearable rob*;
- physical human-rob*, human-robot inter*, phri, pressure, safety;
- measure*, asses*, benchmar*, eval*.

The searches provided a list of 785 publications. After removing duplicated publications and a preliminary review of titles and abstracts, 121 publications were selected for a full text review. A total of 54 publications have been included in this work. The review's flow diagram is depicted in Figure 1.

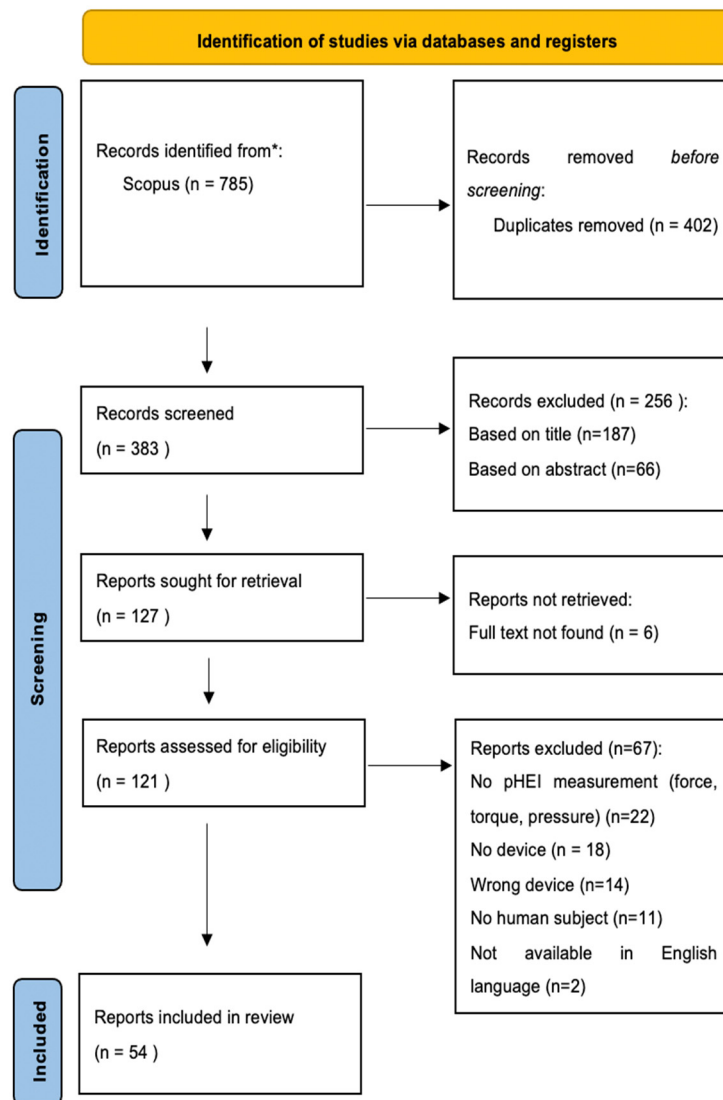


Figure 1. Prisma diagram of the conducted review.

Kinematic or physiologically based metrics such as relative motions, discomfort, and fatigue do not provide direct information of pHEI but rather its consequences on the human body. For this reason, additional kinematic and physiological metrics are included in the results only when supported by pHEI measurements. Other measurements such as Ground reaction forces (GRFs) or Muscle activation (EMG) fell outside the research.

We decided to include both upper limb and lower limb exoskeletons since the proposed solutions can often be shared between the two. For the same reason, both powered exoskeleton, passive exoskeletons, and exosuits have been considered since interaction issues are common among wearable devices. Wrist and hand exoskeletons were excluded from this review since metrics, functions, and evaluations sensitively differ from lower and upper limb exoskeletons.

We classified the papers based on the metric extracted and the sensor solution adopted. The following definitions apply in this paper for pHEI measurement:

- Interaction forces: forces exchanged between the human body and wearable device.
- Interaction torques: torques produced by interaction forces.
- Interaction pressures: pressure calculated from interaction forces over a contact area.

pHEI metrics are classified as follows:

- Force metrics: metrics extracted from interaction force measurement, including normal and shear forces as well as overall interaction force, peak, and average contact force.
- Torque metrics: metrics extracted from interaction torque measurement, normally represented by the single interaction torque generated during the task.
- Pressure metrics: metrics extracted from interaction pressure measurement such as maximum pressure and pressure distribution.

Indirect pHEI metrics were also considered:

- Relative motions: relative motion (in one or more dimensions) between a defined part of the human body and the worn device (frame shift, skin slippage).
- Misalignment: Mismatch in the correspondence in position and orientation between the anatomical and device joint axes.
- Subjective experience metrics (SE): metrics extracted by means of live feedback or questionnaires (Table 1).

3. Results

Of the 54 publications selected, 33 (61%) were published in the last 5 years, from 2016 to 2021 (Figure 2).

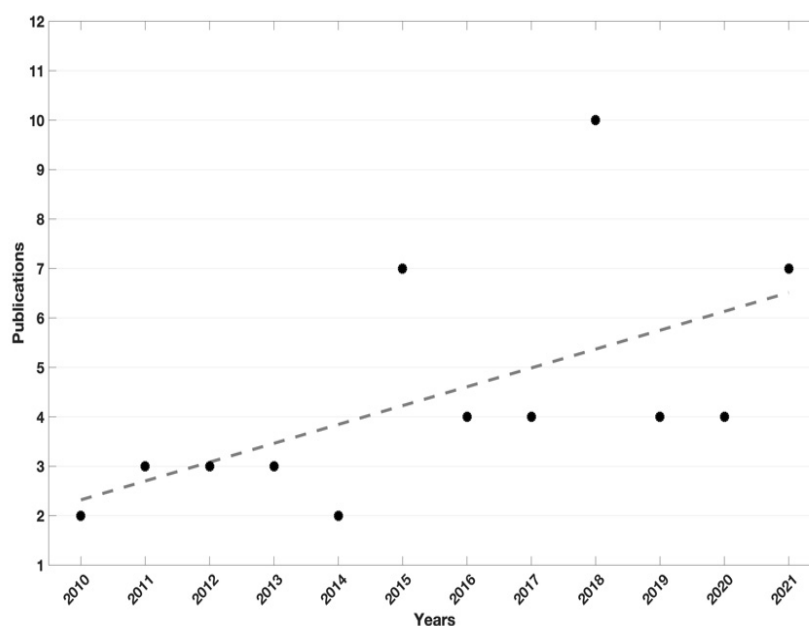


Figure 2. Black dots represents the number of publication per year, dotted line is the black dots trend.

Figure 3 shows the number of publications including each of the considered family of metrics divided into upper and lower limb studies. Interaction was mostly assessed at the lower limbs, with 34 publications (63%) using lower limb devices (including hip exoskeletons and passive leg orthoses) in comparison to the 23 results (42%) obtained for upper body exoskeletons (including shoulder, elbow, and arm support devices). Both groups are counting 3 publications including both upper and lower limb contact measurements. Force-related metrics were preponderant, with 42 publications (78%). Pressure and torque metrics were included in 19 (35%) and 16 (29%) results, respectively. We found a minor

part of the results including supporting pHEI metrics such as user experience (15%), joint misalignments (9%), and relative motions (7%).

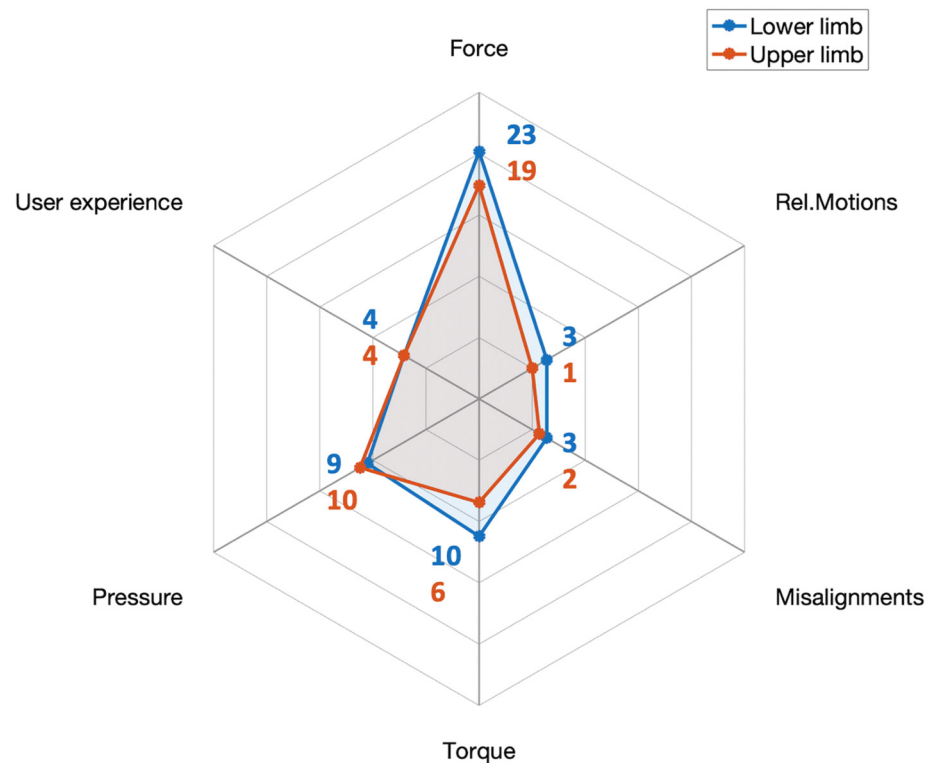


Figure 3. Number of publications including general pHEI metrics divided for upper and lower limb devices.

Metrics from Figure 3 are further detailed, dividing force metrics into overall force metrics, normal (perpendicular to the surface), tangential, and distributed force metrics. The same division is applied for pressure metrics excluding overall pressure since no metrics could fit. Results including these metrics are matched with the relative instrumentation used for their extraction. Figure 4 presents the number of results for each proposed metric, sensor solution, and the intersection between the two axes.

Concerning the instrumentation, load cells (1-axis, 3-axis, and 6-axis) were used in half of the works (26 publications, 48%) to extract force and torque metrics. Optical systems such as fiber optics and laser sensors accounted for 15% of the results. The use of sensors based on force sensing resistors (FSRs) was found in 13 publications (24%), while optical motion tracking systems and air-based pressure sensors (air cushions, pneumatic pads) were found in 13% of the results. Pressure pads different from the above-mentioned technologies were found in 4 studies (7%). The remaining solutions, i.e., strain gauges, goniometers, inclinometers, and capacitive sensors, were found in 16% of the results. Questionnaires were used to extract user-experience metrics and were only considered when pHEI measurements were also included, accounting for 6 publications (11% of the results). Other than questionnaires, visual analog scales (VAS) were also used to extract perceived discomfort [18]. Among the sensor solutions presented in the recordings, 14 (28%) proposed customized sensor solutions for their pHEI measurements [9,18–36]. Most of the developed solutions were FSR-based [19,25,30,33,35] or air-based pressure sensors [18,23,28,29,31]. Optical solutions were divided into optical-fiber sensors [26,27,36] and optoelectronic laser-based sensors [9,20,21]. The remaining solutions were composed of force sensor [22], tactile sensor [24], 3D-printed capacitive sensors [32], and elastic band able to measure interaction through its deformation [34].

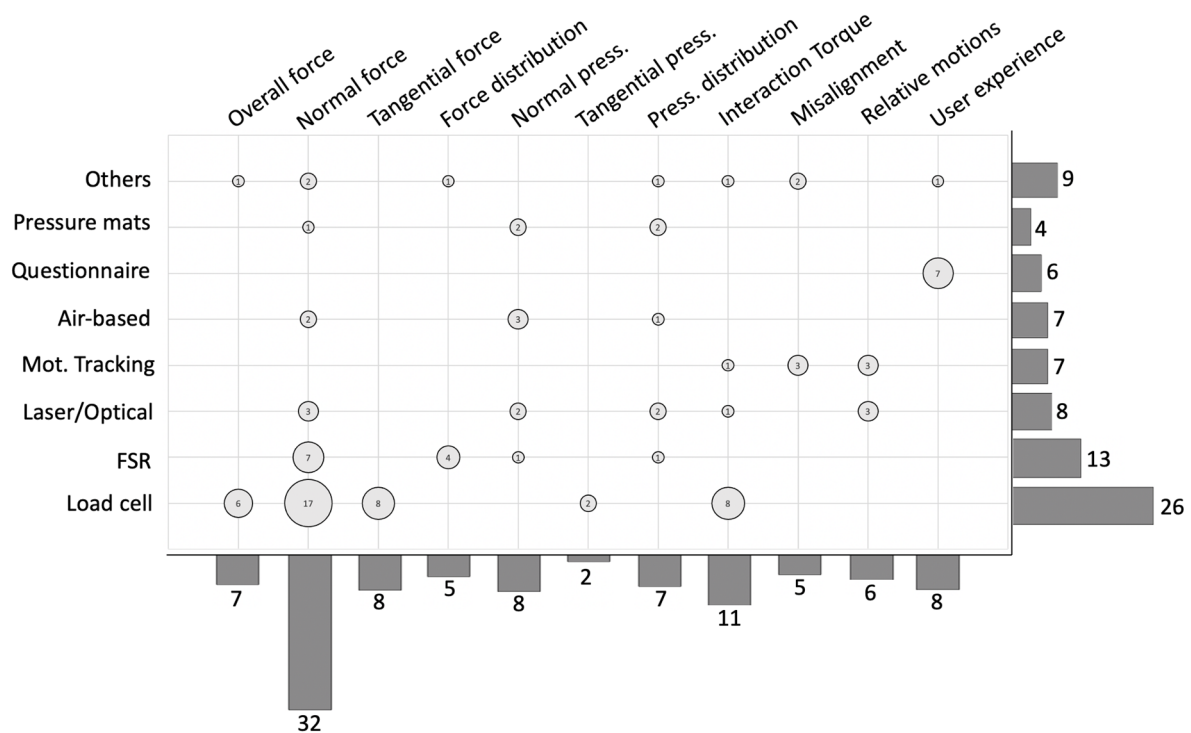


Figure 4. Metrics and sensors solutions in the results. Bar plot on the right represents the number of publications including the listed sensor solutions. Bar plot on the bottom represents the number of publications including the listed metrics. Circles represent the number of studies extracting the relative metric through the relative sensor solution at the intersection.

Force metrics were preponderant, and specifically one-dimensional forces (typically normal to the contact) were generally used for control purposes [19,28,33,37–41] or for contact evaluation strategies such as interface design evaluation [35,42], human–device kinematic compatibility [43,44], misalignment evaluation [31,45–48], or intention detection [40,49]. Normal force metrics were generally the mean absolute value of normal force during the task [18,45,50], force root mean square (RMS) [51–53], average force in a cyclic task [9,39,53–57], peak force [9,58–60], and force range [61]. Normal force mapping allowed the detection of possible areas for interface improvements [24,30,35,42,52].

Normal forces were also used for pressure prediction in new sensory solutions [29]. Torque metrics are normally taken at the joint level to compute interaction torque transferred to the user through the physical interface. Torques can be used in pHEI models to compute how loads are transferred, used for device control [34,38,51,58,62,63], and pHEI prediction and estimation [29,45,46,52,53,64,65]. Pressure measurements were often accompanied by pressure distribution evaluations [20,21,23,25,32,66,67], followed by maximum pressure reached during the task [9,31,55,67,68]. Maximum shear pressure was found only in [56,61], while strapping pressure was also included in a minor part of the results [18,45].

All the studies including pHEI modelling also physically measured pHEI in accordance with our review requirements. The use of models for pHEI evaluation is still limited, with direct measurements being the preferred option. Seventeen results (20%) implemented contact modeling, but 10 of them were for control purposes [37,38,40,41,49–51,54,58,62,63], while 7 results modelled human–device interactions for pHEI prediction or evaluation [18,45,46,52,53,64,65]. Interaction was simply modelled with kinematic parameters for misalignment prediction [46]. Later, human–interface contact was modelled by a spring [45,52] or spring-damper element [18,58,65]. In [64], a more advanced model including the knee angle was needed because the spring damper was found to be insufficient to describe the interaction forces. Nonlinear spring-damper elements were suggested to better describe the contact behavior, at the cost of a higher associated uncertainty [65]. The stiffness and shape of the subject

were claimed to change with motion. Therefore, an improved spring-damper-attitude model including limb position was needed for pHEI modelization in [53].

Twenty-two results (44%) focused on evaluating or improving pHEI safety [18,20,23–25,30,32,42,45,46,50,53,55,56,59,61,64,66–70]. However, 10 of them effectively compared results with safety references [18,20,25,45,55,56,59,66,68,69].

A minor part of these results considered shear pressures [56,61,69], whereas only two studies evaluated and applied safety thresholds [56,69].

Extensive presentation of the results is shown in Table 2, listing results by first author, year of publication, metrics, sensors for their extraction, synthesized protocol applied, device used, and sensorized part of the body.

Table 1. Results including questionnaires with the related extracted metrics.

| Ref. | Questionnaire | Output |
|------|---|--|
| [45] | NASA TLX [71] | Comfort, Physical demand, Mental demand, Temporal demand, operator performance, Effort |
| [47] | Custom Borg scale [72] | Perceived comfort, Physical load |
| [54] | Custom | Comfort, interface preference |
| [55] | Custom | Comfort |
| [70] | Custom | Safety |
| [68] | Borg category ratio (CR-10) [72] Van der Grinten and Smitt System Usability Scale (SUS) | Perceived musculoskeletal effort (arm, trunk, leg) Local Perceived Pressure (back/shoulders, arms, chest, and belly/hips) Usability of the exoskeleton |

Table 2. Review summary. IF: interaction force, IT: interaction torque, IP: interaction pressure, n.a.: not applicable.

| Author and Ref. | Year | pHEI Metrics | Sensor | Protocol | Device | Sensor Placement |
|---------------------|------|--|--|---------------------------|--|------------------------|
| Akyiama et al. [46] | 2012 | IF/support metrics: Normal force, Misalignment | Load cell 3D motion capture system | n.a. | Lower limb exoskeleton frame mounted on a dummy leg | Lower leg Upper leg |
| Akyiama et al. [64] | 2015 | IF/support metrics: Normal/Tangential IF, Relative motions | 3-axis Load cell 3D optical motion capture system | 10 sit-to-stand motions | Leg type motor-actuated lower-limb orthosis | Lower leg Upper leg |
| Akyiama et al. [69] | 2012 | IF/IT/support metrics: Normal/Tangential IF, Interaction moment, Skin slippage, Relative motions | 3-axis Load cell Slip sensor (2D imaging devices) 3D optical motion capture system | 15 sit-to-stand motions | Lower limb physical assistant robot | Upper leg |
| Amigo et al. [48] | 2012 | IF/support metrics: Normal/Tangential IF, Misalignment | 6-axis Load cell Full bridge strain gauges | Forearm flexion-extension | Arm orthoses | Forearm |

Table 2. Cont.

| Author and Ref. | Year | pHEI Metrics | Sensor | Protocol | Device | Sensor Placement |
|-----------------------------|------|--|--|---|--|-------------------------------------|
| Awad et al. [70] | 2020 | IF/support metrics: Disturbing force, Adverse event observation, Patient feedback | Load cell Questionnaire | 20 min of overground walking practice, 20 min of treadmill walking practice | Lower limb soft exosuits | Not specified |
| Beil et al. [40] | 2018 | IF: Overall 3D IF | 3-axis Load cell | 13 different motion tasks | Lower limb exoskeleton | Upper leg Lower leg |
| Bartenbach et al. [47] | 2015 | IF/support metrics: Overall IF, Misalignments, Perceived discomfort, Physical load | Load cell 3D optical motion capture system Questionnaire | 2 min of familiarization and 20 s of test on a treadmill | Lower limb exoskeleton | Lower leg Upper leg |
| Bessler et al. [30] | 2019 | IF/IT: Normal/Tangential IF, Force distribution, Interaction torque | FSR sensor 3-axis load cell | Moving forearm along 3 axis | Forearm support | Forearm |
| Choi et al. [19] | 2018 | IF: Normal force | FSR sensor | Treadmill walking | Hip exoskeleton | Thigh |
| Christensen et al. [43] | 2018 | IF: Normal force | FSR sensor | n.a. | 3DOF spherical mechanism for shoulder joint exo | Arm Forearm |
| Del-ama et al. [39] | 2011 | IF/IT: Mean interaction force Mean interaction torque (calculated) | Gauge bridge | 10 min leg swing | Lower limb exoskeleton | Lower leg |
| De Rossi, Lenzi et al. [21] | 2010 | IP: Pressure distribution | Matrix of optoelectronic sensors | treadmill walk at 4 Km/h in 3 different conditions: “no-assistance” “low-assistance” and “high-assistance” | Lower limb robotic platform | Upper leg Lower leg |
| Donati, De rossi et al. [9] | 2013 | IF/IP: Average IF, Maximum IF, Maximum IP | Load cell Matrix of optoelectronic sensors | Upper limb: Passive arm Active arc Lower limb: Transparent mode Viscous field | Elbow active orthoses Lower limb robotic platform | Forearm Upper leg Lower leg |
| Fan et al. [58] | 2013 | IF: Max normal IF, Normal IF | Airbags sensor | knee extension to 30° and 60° | Lower limb exoskeleton | Calf |
| Georgarakis et al. [61] | 2018 | IF/IP: Normal/tangential IF range, Max normal/tangential IF, Shear IP range | 3-axis Force sensor | relax or contract the forearm muscles by grasping a handle according to different force pattern | Upper limb exoskeleton | Forearm |
| Ghonasgi et al. [35] | 2021 | IF: Force distribution | FSR sensor matrix | Elbow extensions | Upper limb exoskeleton | Upper arm |
| Grosu et al. [22] | 2017 | IF: Normal force | 3-axis Force sensor | n.a. | Lower limb exoskeleton | Hip |
| Hasegawa et al. [23] | 2011 | IP: Pressure distribution | Active air mat | Arm suspended Arm moving Arm lifting a weight | Upper limb exoskeleton | Forearm |
| Huang et al. [38] | 2015 | IF: Total normal force over 4 point | FSR sensor | n.a. | Upper limb power-assist robotic exoskeleton | Forearm |
| Huysamen et al. [68] | 2018 | IP/support metrics: Maximum pressure, Local perceived pressure, Subjective usability | Pressure mat Questionnaires | Lifting a load from the ground, with/without device, with/without load | Back powered exoskeleton | Shoulder Hip/lower back Thigh |

Table 2. Cont.

| Author and Ref. | Year | pHEI Metrics | Sensor | Protocol | Device | Sensor Placement |
|-------------------------|------|--|--|--|----------------------------------|--------------------------|
| Islam et al. [33] | 2019 | IF: Normal force variation | FSR sensor band | Arm liftingh with different payloads | Passive arm exoskeleton | Upper arm |
| Ito et al. [24] | 2018 | IF: Force distribution | Tactile sensor | n.a. | Wearable robot for upper limb | Upper arm |
| Kim et al. [57] | 2013 | IF: Average normal IF | Load cell | Walking on a mat | Prototype lower limb exoskeleton | Shank |
| Kim et al. [31] | 2021 | IP/support metrics: Maximum pressure, Average normalized IP, Misalignment | Air-bladder pressure sensor 3D optical motion capture system | Knee flexion-extension using a pulling cable attached to the foot | Lower limb exoskeleton | Shank |
| Langlois et al. [18] | 2020 | IF/IP/support metrics: Normal IF, Strapping pressure, Relative motions, Energy dissipation, Perceived comfort | Air cushion 3D optical motion capture system Visual analog scale | randomly chosen motions at 5 different inflation pressure | 7 DOF robotic manipulator | Arm |
| Langlois et al. [32] | 2021 | IP: Pressure distribution | 3D printed capacitive sensor pads | Lifting weights with arm straight | Upper arm interface | Arm |
| Leal-junior et al. [26] | 2018 | IT: Lifting torque | Optical fiber sensor Potentiometer | Free knee flexion and extension | Lower limb exoskeleton | Shank |
| Leal-junior et al. [27] | 2018 | IF: Normal force | Optical fiber sensor (Bragg) | Free knee flexion and extension | Lower limb exoskeleton | Shank |
| Leal-junior et al. [36] | 2019 | IF: Normal force | Optical fiber sensor Load cell | Free knee flexion and extension | Lower limb exoskeleton | Calf |
| Lee et al. [41] | 2014 | IF: Normal/Tangential IF | Load cell | Arm lifting at different load conditions | Upper limb exoskeleton | Handle |
| Lenzi et al. [20] | 2011 | IP: Normal IP, Pression distribution | Matrix of optoelectronic sensors | 1. leaving arm passive; 2. moving faster (higher frequency) than the robot; 3. moving slower than the robot; 4. imposing higher flexion angle than the robot; 5. imposing a higher extension angle than the robot. | Elbow active orthoses | Forearm |
| Levesque et al. [42] | 2017 | IF: Force distribution | FSR matrix sensor FSR sensor | legged deep squats, lunges, as well as stair climb and descent | Lower limb exoskeleton | Thigh Knee Tibia |
| Li et al. [44] | 2019 | IF/IT: 3-D IF, Normalized IF over 3-axis, 3-D IT, Normalized IT over 3-axis | 6-axis Load cell | Walking on treadmill | Prototype lower limb exoskeleton | Upper limb Lower limb |
| Lobo-prat et al. [54] | 2016 | IF/support metrics: Average normal IF, Comfort | Load cell EMG Questionnaire | Elbow flexion-extension movements against gravity | Passive upper limb support | Handle |
| Long et al. [34] | 2017 | IT: Interaction torque | Elastic band | Leg swings in the air | Lower limb exoskeleton | Thigh and calf |

Table 2. Cont.

| Author and Ref. | Year | pHEI Metrics | Sensor | Protocol | Device | Sensor Placement |
|----------------------------|------|---|---|---|------------------------------------|----------------------------|
| Long et al. [49] | 2017 | IP: Contact pressure | Pneumatic gas-bag | 40 m walk with (1) passive exo, (2) active exo without gravity compensation, (3) active exo with gravity compensation | Lower limb exoskeleton | Upper leg Lower leg |
| Long et al. [63] | 2018 | IT: Interaction torque | Torque sensor | Natural speed of about 0.8 m/s and the maximum velocity up to 4 km/h with 30 kg loads | Lower limb exoskeleton | Knee |
| Mahdavian et al. [37] | 2015 | IF: Normal IF | Strain gauges | n.a. | Prototype upper limb exoskeleton | Elbow |
| Masud et al. [50] | 2021 | IF/(IT) Module magnitude of normal IF, Calculated IT | 6-axis Load cell | n.a. | Arm exoskeleton | Lower arm |
| Muozo et al. [65] | 2020 | IT: Bending torque | Load cell 3D optical motion capture system | Normal walking with locked Orthotic knee and actuated Orthotic knee | Leg orthoses | Knee |
| Quinlivan et al. [66] | 2015 | IP: Pressure distribution | Pressure mat | n.a. | Soft exosuit | Thigh Hip Belly |
| Rathore et al. [59] | 2016 | IF: Maximum normal IF | FSR sensor | two steps forward (a full gait cycle) | Lower limb exoskeleton | Thigh braces Leg braces |
| Schiele et al. [45] | 2010 | IF/IT/IP/support metrics: Mean absolute normal IF, Mean absolute IT, Fixation cuff IP, Tracking error, Subjective comfort and workload, Misalignments | 6-axis Load cell Pressure interface Questionnaire | visually track a random target on a screen | Upper limb exoskeleton | Forearm |
| Tamez-Duque J. et al. [25] | 2015 | IP: Normal pressure, Pressure distribution | FSR pressure pad | sit to stand, walk forward, turn 180° to the right, turn 180° to the left, stand to sit | Lower limb exoskeleton | Upper leg Lower leg |
| Tran et al. [62] | 2014 | IT: Interaction torque | Torque sensor Inclinometer | n.a. | Lower limb exoskeleton | Knee |
| Tran et al. [51] | 2021 | IF/IT: Normal IF, Performance index: normalized square sum of the sagittal plane IF | 2-axis Force sensor | n.a. | Lower limb exoskeleton | Thigh Shank |
| Wan et al. [56] | 2020 | IF/IP/support metrics: Average normalized IF (normal + shear), Maximum shear stress, Human-cuff relative motion, Cuff slip velocity | 3-axis Force sensor Laser mouse sensor | Walking on treadmill | Custom-made lower limb exoskeleton | Thigh Calf |
| Wang et al. [55] | 2020 | IF/IP/support metrics: Average normal force, Maximum normal pressure, Comfort | FSR sensor Questionnaire | 10 repetitions of sit-to-stand, standing for 10 min, walking for 10 m, and stand-to-sit | Lower limb exoskeleton | Shin Hands |
| Wang et al. [28] | 2021 | IF: Overall IF | Soft pneumatic force sensor | Walking on treadmill | Hip exoskeleton | Thigh |

Table 2. Cont.

| Author and Ref. | Year | pHEI Metrics | Sensor | Protocol | Device | Sensor Placement |
|------------------------|------|---|--|--|---------------------------------------|--------------------|
| Wilcox et al. [60] | 2016 | IF: Average peak force | FSR sensor EMG | Two steps forward Two steps backward Two sidesteps | Lower limb exoskeleton | Thigh Lower leg |
| Wilkening et al. [29] | 2016 | IF/IT/IP Normal IF Interaction torque Normal pressure | Pneumatic pad 6-axis Load cell | n.a | Forearm interface | Forearm |
| Xiloyannis et al. [67] | 2018 | IF/IT/IP Normal IF Interaction torque, Pressure distribution, Pressure peak | Pressure pad | Three flexion/extension movements between 0° and 90° | Elbow exosuit | Elbow |
| Yousaf et al. [52] | 2021 | IF: Normal distribution, Average RMS normal distribution | 6-axis Load cell FSRs | n.a. | Upper arm exoskeleton interface | Arm |
| Zanotto et al. [53] | 2015 | IF/IT: Average normal IF, RMS normal IF, Average IT | 6-axis Load cell Potentiometric goniometer | Treadmill walking in inertia, velocity, and alignment conditions | Treadmill-based exoskeleton | Thigh Shank |

4. Discussion

Research in pHEI has been growing in the last years together with the necessity to properly address safety issues in wearable robots. However, the gap between the current knowledge and the need for data-based evidence to test and prove the level of safety in the current growing market is still huge. So far, the great variability of pHEI assessment methods, devices, and applications has prevented their harmonization. The need for a more standardized way to evaluate the safety of human–exoskeleton contact issues is becoming urgent. In this section, we summarize the main metrics found for pHEI measurement, discussing their implementation and the challenges in building links between measurements and safety.

4.1. pHEI Metrics and Measurements

Force was the principal quantity extracted to address pHEI, typically assessed in a normal direction with the body (normal interaction force).

Maximum normal force is typically used to assess and evaluate new solutions by monitoring their ability to decrease force magnitude. However, if the residual interaction is safe for the user, it is usually not addressed [44,59]. Tangential, or shear, forces can be extracted together with the normal component adding important information about the contact, being responsible for twisting and tearing the user’s skin, which can produce discomfort and skin injuries [73]. Metrics including shear forces can be monitored to inform interaction quality and power transfer efficiency, although some sensor solutions cannot properly address their contribution in the overall interaction. FSR-based solutions were never characterized with tangential interaction while other solutions simply recorded the overall interaction force (pneumatic/air-based sensors). Shear contribution was generally rarely analyzed.

Force and torque metrics were also included in interaction models for control and pHEI prediction. Human body parameters can drastically change among subjects and body sites [18]. Results are affected by individuality [56], making model robustness one of the major challenges in the field. Model complexity and limited reproducibility of exoskeleton tasks prevents them from reaching accurate predictions outside the experimented scenario, thus limiting the findings to the single tests [32,64] and leading to a preference for simpler models [52,65]. However, we consider research on pHEI modelization to be important since

the pHEI sensory system is often applicable for specific conditions, and new knowledge from modelization would allow pHEI predictions and monitoring through a set of standard sensors outside the testing phase.

From this perspective, only a limited portion of the results considered pressure measurements and related metrics. Difficult contact area estimation and expensive solutions still prevent the community from attaining comprehensive knowledge of interaction pressure. Pressure measurements were often related to the study of distribution and how they vary with time and motion. How this pressure changes in time and space during the motion, however, is still not fully addressed. Dividing tangential from perpendicular interaction is generally difficult, and the real contribution of each component is often unknown [31]. The lack of evidence of human limits under shear stress together with the technological challenges resulted in a very restricted number of publications including shear pressures [56,61]. Both results extracted shear pressure by dividing tangential forces over an estimated contact area. At the current state of the art, no solution was found that could provide shear pressure output. This result shows how research in this field is influenced by technological limitations. Independently from the growth and interest in the field, we consider that facing the complex contact behaviour at the interface represents one of the main factors hampering new findings in pHEI. Calibration with shear forces is normally difficult and performed on flat and rigid surfaces. Interaction on soft human tissues introduces serious challenges in terms of test reproducibility sensor positioning and output calibration that hamper the development of a clear setup for pHEI evaluation. Any new attempt in this direction can produce precious and unexplored knowledge of how human–exoskeleton contact is characterized, and what the implications are during contact safety evaluation. At the time of this review, efforts in this direction are still limited.

Other metrics can inform the quality and safety level of the interaction, but their meaning needs to be clarified through pHEI measurements (e.g., forces, torques, pressures) since they do not provide direct information on the physical contact. Relative motions can describe how efficiently power can be transmitted from the device to the user's biological structures [74]. This information is usually extracted through optical systems. A few exceptions are represented by laser sensors monitoring skin slippage and velocity [64,69].

Other kinematic metrics, such as human–exoskeleton joint misalignments, are responsible for undesired shear forces at the interface. Misalignments represent an important field of study. They can achieve the order of ± 10 cm in various directions, even if at the start of the movement joints are well aligned [45]. Misalignments cause frame shifts and limit the voluntary range of motion, especially in larger motions, together with the generation of undesired forces. However, a clear linear dependence between misalignments and force is not always observed, suggesting a more complex relationship. A proper misalignment definition will be evaluated by checking both the 3-D position and angular alignment between the joint centres, although they are often reduced to a single plane. At the state of the art, no results were found considering joint misalignments in the 3D space. Defining the degree of relevance of the different planes/directions will be an issue for future studies. The same considerations apply to relative motions and slippage since they are always measured taking into account fewer dimensions and plans.

We consider that the relationship between kinematic metrics and forces will be matters of further investigation in future studies. The possibility of informing some safety aspects by means of kinematic measurements may represent a promising approach in the field of pHEI, preventing the experimenters from dealing with the difficulties of force/pressure measurements.

Nevertheless, strong preliminary studies are first needed to support pHEI evaluations through kinematic metrics, and few efforts were found in this direction.

User experience assessment is normally conducted using questionnaires and open feedback from users. Typical metrics were perceived pressure, comfort, and safety during the task. Their assessment, together with pHEI measurements, can provide useful links between subjective and physical metrics in the effort to find physiological limits associated

with safety. We could not find any publication linking physical metrics with perceived pain or discomfort during an exoskeleton task. User experience metrics were mainly used as feedback for the assessment of the device or the additional mechanism applied.

With regard to the sensing systems, load cells were often included for force measuring. Depending on the available degrees of freedom, load cells can extract different metrics such as normal interaction force (using 1-3-6 axis load cell), shear forces (3-6 axis load cell), and interaction moments (6 axis load cell). Load cells do not require particular models but do not allow a comprehensive quantification of how pHEI is distributed at the contact area, providing a limited representation of the overall behaviour. Load cells were normally integrated in the exoskeleton itself, thereby reducing the setup flexibility and applicability to other devices. An alternative solution to overcome the issue of force distribution was found in FSR-based sensors. Their main advantages are the reduced cost and the possibility to be comfortably placed at the contact points without affecting the user comfort. However, these solutions often suffer from drift caused by prolonged pressure and remain less suitable for bending and tearing. They need to be manually calibrated after placement and can only estimate normal forces. On the other side, thanks to their limited and known area, they have been used to map pressure distribution at the interfaces. Nevertheless, they can also suffer from poor repeatability, thus raising some concerns regarding their extensive use in pHEI applications.

Commercial sensors based on FSR technology could guarantee higher performance compared with customized solutions. Additionally, commercial solutions can often offer a more comfortable hardware wearing, limiting wiring and electronic devices. Their main drawback is their generally higher cost and more complex integrability in a wider experimental setup. Furthermore, attention will be paid to evaluating the comfort–pressure relation when adding pressure mats as they introduce additional stiffness that can sensitively change the perceived comfort between limb and interface [66]. An alternative and promising solution was represented by air-based sensors, such as pneumatic padding and air cushions [18]. These solutions can be inflated at the desired pressure, thus monitoring their compliance and providing absolute pressure value independently of the load direction. In this way, not only normal interaction pressure but the overall interaction can be recorded without the need for complicated calibration procedures. All air-based solutions in the literature were developed and built by the experimenters for the published applications. No commercial solutions were applied in the results.

A discrete number of publications developed customized sensor solutions, which highlights the lack of commercially available solutions able to meet the requirements and needs of pHEI assessment. Most of the solutions were based on FSR and pneumatic/air-based pressure sensors. While air-based solutions can rely on stronger and repeatable calibrations, they also require a certain space to be positioned between the human limb and the device. Their positioning results in less transparency and could strongly affect the perceived comfort of the user at the test execution. FSR introduces the advantages of a more adjustable and flexible shape and size, together with a reduced price. We consider FSR solutions to have found more applications in the interaction distribution measurement, but they are less reliable in providing an accurate and repeatable output, although this lack could be filled by air-inflatable solutions. Different solutions were limited. Optical-based solutions were fibre-optic sensors and optoelectronic laser pads, but their development was limited to two different authors. Among the remaining technologies, 3D-capacitive sensors could represent a valuable technology for future research given their adaptability and the advantages of the capacitive technologies with respect to FSRs in terms of hysteresis and robustness.

4.2. Safety Evaluation

The problem of assessing safety in pHEI remains related to the necessity to properly measure and evaluate the force–pressure exchanged, creating a link between the recorded data and the safety of the contact evaluated. Typically, no specific metrics are described

when normal interaction is used for control purposes or for custom sensor validation. Instead, specific metrics are usually found in studies focusing on safety, although information of a singular force component is normally insufficient to address safety. Safety cannot be properly addressed by force and torque metrics, since they do not normally include information on the contact area. The contact safety is evaluable when both the force and contact area are known; thus, pressure metrics need to be included when safety considerations are performed [75].

Accepted metrics in the literature linking pressure with pain and discomfort are: (i) the pressure magnitude at which the pain occurs (pain detection threshold, PDT), and (ii) the pressure magnitude that causes unbearable pain (pain tolerance threshold, PTT) [76]. However, these metrics suffer several influencing factors such as skin condition, age, gender, stimulus, and body site that concur in making the finding of clear pass/fail criteria very challenging.

Typical tests for PDT/PTT definition concern normal loads and static contacts for medical purposes. The subjects are stimulated either in a single point (single point algometry) or on a surface (computerized pressure algometry) [76–81]. Due to this evidence, most of the results in this review concerning safety verification considered normal loads and referred to the mentioned tests in the literature [18,20,25,45,55,56,59,66,68,69].

However, both normal and tangential force components contribute to contact safety [73]. Shear stresses are thought to act in conjunction with normal pressure to produce the damage. From the literature, we know how in the presence of high shear forces, half the normal force normally required for blood vessel occlusion was enough to produce the same effects [82–86]. Shear stresses not only act to decrease the bearable normal pressure level but also concur in blister generation under repetitive rubbing [87].

Despite the fact that soft tissue damage was consistently present in different reviews of adverse events [88], hazards [89], and risk management [90] for lower limb exoskeletons, research on shear stresses is still very limited. Records considering shear pressures and their limit for human safety were sensitively limited.

A shear stress–time relation was already proposed [91], underlying the dependence of the pressure's effect with time. The importance of considering exposure time together with interaction magnitude lead to the development of safety tests for physical assistant robots [92,93], later adopted in ISO TR 24482-1 [75]. Perceived pressure was also suggested to increase with time, providing different results for ergonomic evaluations [68].

Contrary to this trend in the literature, the collected records compared their results with pressure limits from single point algometry methods, which are appropriate for concentrated rather than distributed loads. FSR arrays were used for pressure contact measurements [25,55], claiming how interaction remained much lower than PTT in the literature [25,55,59,68]. However, inconsistencies between perceived pain and PTT threshold were also experienced [55,68]. Furthermore, the use of PTT seems improper in exoskeletons since it is related with unbearable pain, whereas exoskeletons are devices meant to be used for a prolonged period of time.

PDT/PTT-targeted for exosuits were collected through a visual analog scale (VAS) and questionnaires from the participants to inform design specifics [94]. PDT in calves, thighs, and knees spanned from 21.4 kPa to 90.3 kPa, while PTT in the same locations was assessed from 49.6 kPa to 90.3 kPa. In the context of safety, the use of pressure rather than force thus appears more justified since all the available discomfort and pain limits are presented in a pressure scale. PDT and PTT limits overlapped considerably; thus, the effectiveness of the aforementioned pressure ranges will be better explored in real exoskeleton tasks and supported by further evidence.

Variability issues of pressure limits were also experienced at the strapping pressure, and were rarely properly considered. Initial strapping pressure was adjusted at a level considered comfortable for the subjects. However, although both studies considered upper limb exoskeletons, maximum strapping pressure was set at 14 kPa for [18], while the referred ideal pressure was set at 2.6 kPa in [45].

These inconsistencies suggest that different devices might need different strapping forces to guarantee user comfort during the task. If we look at lower limbs, 133 kPa [25] was considered an acceptable pressure, thus suggesting that different interaction pressure studies will be performed for different device families. One more consideration is needed when patients are included in the task. One of the main scopes of an exoskeleton is to assist patients, and physical limits cannot be generalized considering the literature on healthy subjects. From this point of view, only two results in this review included spinal cord injury, SCI patients [25,65], and only one focused on pHEI measurements for safety interaction assessment [25], thereby showing how pressure recorded in SCI patients was greater than healthy patients.

Subject, device, and task seem to highly influence the interaction output, preventing the finding of more generalized safety limits. Still, few studies have been conducted in the field of exoskeletons, leaving a research gap that will be addressed together with exoskeleton development.

5. Conclusions

This review summarized the most relevant publications focusing on the assessment of physical human–exoskeleton interaction (pHEI) in the last 10 years.

Apart from the increasing interest of the community in this topic, we identified a clear gap in the definition of protocols and procedures to assess pHEI.

Proposed methods suffer a great variability of tests, protocols, subjects, and setup conditions, making their relationship with human safety limits unclear. The proper, objective, and reproducible study of pHEI could represent a crucial step forward in the field of safety evaluation in wearable robots. Here, studying how the interaction is distributed at the contact points between the human and the robot should be a matter of additional attention from the community. Future studies should consider improving test reproducibility and setup flexibility to cover a wider range of devices and allow harmonization and test comparisons. More solid knowledge of the effect and characterization of interaction pressure is now needed to build protocols that can be applied not only to the single device in a study but to a device family. Additional future efforts should also clarify the effectiveness of kinematic metrics to be used as safety-related indicators.

This review can help researchers understand the current challenges in the assessment of exoskeleton safety and promote cooperative work within the community to find agreed-upon testing methodologies and metrics to properly assess the quality of the existing physical interaction between humans and exoskeletons.

Author Contributions: Conceptualization, S.M., D.P.-F. and D.T.; Investigation, writing—original draft preparation, S.M.; writing—review and editing, D.P.-F., D.R.-C., D.T. and M.L.; supervision, D.R.-C., J.C.M., D.T. and M.L. All authors have read and agreed to the published version of the manuscript.

Funding: This work was funded by the European project EXOSAFE (agreement No. RRD7218.02.02), an awarded project by the COVR project, funded by the European Union’s Horizon 2020 research and innovation programme under grant agreement No. 779966.

Institutional Review Board Statement: Not applicable.

Informed Consent Statement: Not applicable.

Data Availability Statement: Not applicable.

Conflicts of Interest: The authors declare no conflict of interest.

References

1. Peters, M.; Wischniewski, S. *Impact of Using Exoskeletons on OSH*; Discussion Paper; European Agency for Safety and Health at Work: Bilbao, Spain, 2019; pp. 1–10.
2. Spada, S.; Ghibaudo, L.; Gilotta, S.; Gastaldi, L.; Cavatorta, M.P. Investigation into the Applicability of a Passive Upper-Limb Exoskeleton in Automotive Industry. *Procedia Manuf.* **2017**, *11*, 1255–1262. [[CrossRef](#)]

3. van der Vorm, J.; Nugent, R.; O'Sullivan, L. Safety and Risk Management in Designing for the Lifecycle of an Exoskeleton: A Novel Process Developed in the Robo-Mate Project. *Procedia Manuf.* **2015**, *3*, 1410–1417. [[CrossRef](#)]
4. Jhavar, V. Design of a Knee Exoskeleton for Gait Assistance. *J. Chem. Inf. Model.* **2013**, *53*, 1689–1699. [[CrossRef](#)]
5. Alami, R.; Albu-Schaeffer, A.; Bicchi, A.; Bischoff, R.; Chatila, R.; De Luca, A.; De Santis, A.; Giralt, G.; Guiochet, J.; Hirzinger, G.; et al. Safe and Dependable Physical Human-Robot Interaction in Anthropic Domains: State of the Art and Challenges. In Proceedings of the 2006 IEEE/RSJ International Conference on Intelligent Robots and Systems, Beijing, China, 9–15 October 2006. [[CrossRef](#)]
6. Norm, D. *ISO 13482; Safety Requirements for Personal Care Robots*. ISO: Geneva, Switzerland, 2008; ISBN 9362178001.
7. Massardi, S.; Pinto-Fernandez, D.; FVeneman, J.; Torricelli, D. Testing Safety of Lower Limbs Exoskeletons: Current Regulatory Gaps. In *International Symposium on Wearable Robotics*; Springer: Cham, Germany, 2020; pp. 145–149.
8. Villaronga, E.F. New Trends in Medical and Service Robots. In *Mechanisms and Machine Science*; Springer: Berlin/Heidelberg, Germany, 2016; Volume 39, p. 59972. [[CrossRef](#)]
9. Donati, M.; Vitiello, N.; de Rossi, S.M.M.; Lenzi, T.; Crea, S.; Persichetti, A.; Giovacchini, F.; Koopman, B.; Podobnik, J.; Munih, M.; et al. A Flexible Sensor Technology for the Distributed Measurement of Interaction Pressure. *Sensors* **2013**, *13*, 1021–1045. [[CrossRef](#)]
10. Sposito, M.; Toxiri, S.; Caldwell, D.G.; Ortiz, J.; De Momi, E. Towards Design Guidelines for Physical Interfaces on Industrial Exoskeletons: Overview on Evaluation Metrics. *Biosyst. Birobot.* **2019**, *22*, 170–174. [[CrossRef](#)]
11. Chen, B.; Ma, H.; Qin, L.Y.; Gao, F.; Chan, K.M.; Law, S.W.; Qin, L.; Liao, W.H. Recent Developments and Challenges of Lower Extremity Exoskeletons. *J. Orthop. Transl.* **2016**, *5*, 26–37. [[CrossRef](#)]
12. Rodríguez, C.A.C.; José, Á.; Perez, B.; Múnera, M.; Arévalo, A.S.; García, C.A.C. *Biomechanical Assessment of a Lower Limb Exoskeleton*; IX Congreso Iberoamericano de Tecnología de Apoyo a la Discapacidad: Bogotá, Colombia, 2017; pp. 416–423.
13. Nabeshima, C.; Kawamoto, H.; Sankai, Y. Strength Testing Machines for Wearable Walking Assistant Robots Based on Risk Assessment of Robot Suit HAL. In Proceedings of the 2012 IEEE International Conference on Robotics and Automation, Saint Paul, MN, USA, 14–18 May 2012; pp. 2743–2748. [[CrossRef](#)]
14. Zeilig, G.; Weingarden, H.; Zwecker, M.; Dudkiewicz, I.; Bloch, A.; Esquenazi, A. Safety and Tolerance of the ReWalk™ Exoskeleton Suit for Ambulation by People with Complete Spinal Cord Injury: A Pilot Study. *J. Spinal. Cord. Med.* **2012**, *35*, 96–101. [[CrossRef](#)]
15. Kolakowsky-Hayner, S.A. Safety and Feasibility of Using the Ekso™ Bionic Exoskeleton to Aid Ambulation after Spinal Cord Injury. *J. Spine* **2013**, *43*, 657–666. [[CrossRef](#)]
16. Huysamen, K.; Bosch, T.; de Looze, M.; Stadler, K.S.; Graf, E.; O'Sullivan, L.W. Evaluation of a Passive Exoskeleton for Static Upper Limb Activities. *Appl. Ergon.* **2018**, *70*, 148–155. [[CrossRef](#)]
17. Meyer, J.T.; Schrade, S.O.; Lambercy, O.; Gassert, R. User-Centered Design and Evaluation of Physical Interfaces for an Exoskeleton for Paraplegic Users. In Proceedings of the 2019 IEEE 16th International Conference on Rehabilitation Robotics (ICORR), Toronto, ON, Canada, 24–28 June 2019; pp. 1159–1166. [[CrossRef](#)]
18. Langlois, K.; Rodriguez-Cianca, D.; Serrien, B.; De Winter, J.; Verstraten, T.; Rodriguez-Guerrero, C.; Vanderborght, B.; Lefeber, D. Investigating the Effects of Strapping Pressure on Human-Robot Interface Dynamics Using a Soft Robotic Cuff. *IEEE Trans. Med. Robot. Bionics* **2020**, *1*, 146–165. [[CrossRef](#)]
19. Choi, H.; Seo, K.; Hyung, S.; Shim, Y.; Lim, S.C. Compact Hip-Force Sensor for a Gait-Assistance Exoskeleton System. *Sensors* **2018**, *18*, 566. [[CrossRef](#)]
20. Lenzi, T.; Vitiello, N.; De Rossi, S.M.M.; Persichetti, A.; Giovacchini, F.; Roccella, S.; Vecchi, F.; Carrozza, M.C. Measuring Human-Robot Interaction on Wearable Robots: A Distributed Approach. *Mechatronics* **2011**, *21*, 1123–1131. [[CrossRef](#)]
21. De Rossi, S.M.M.; Vitiello, N.; Lenzi, T.; Ronsse, R.; Koopman, B.; Persichetti, A.; Giovacchini, F.; Vecchi, F.; Ijspeert, A.J.; Van Der Kooij, H.; et al. Soft Artificial Tactile Sensors for the Measurement of Human-Robot Interaction in the Rehabilitation of the Lower Limb. In Proceedings of the 2010 Annual International Conference of the IEEE Engineering in Medicine and Biology, Buenos Aires, Argentina, 31 August–4 September 2010; pp. 1279–1282. [[CrossRef](#)]
22. Grosu, V.; Grosu, S.; Vanderborght, B.; Lefeber, D.; Rodriguez-Guerrero, C. Multi-Axis Force Sensor for Human-Robot Interaction Sensing in a Rehabilitation Robotic Device. *Sensors* **2017**, *17*, 1294. [[CrossRef](#)]
23. Hasegawa, Y.; Tayama, M.; Saito, T.; Sankai, Y. Active Air Mat for Comfortable and Easy to Wear a Forearm Support System. In Proceedings of the 2011 IEEE/RSJ International Conference on Intelligent Robots and Systems, San Francisco, CA, USA, 25–30 September 2011; pp. 4899–4904. [[CrossRef](#)]
24. Ito, D.; Funabora, Y.; Doki, S.; Doki, K. Prototype of Wearable Robot with Tactile Sensor Measurable Contact Force Distribution with User. In Proceedings of the 2018 15th International Conference on Control, Automation, Robotics and Vision (ICARCV), Singapore, 18–21 November 2018; pp. 960–965. [[CrossRef](#)]
25. Tamez-Duque, J.; Cobian-Ugalde, R.; Kilicarlan, A.; Venkatakrisnan, A.; Soto, R.; Contreras-Vidal, J.L. Real-Time Strap Pressure Sensor System for Powered Exoskeletons. *Sensors* **2015**, *15*, 4550–4563. [[CrossRef](#)]
26. Leal-Junior, A.G.; Frizzera, A.; Marques, C.; Pontes, M.J. Development of Polymer Optical Fiber Sensors for Lower Limb Exoskeletons Instrumentation. *Biosyst. Birobot.* **2019**, *22*, 155–159. [[CrossRef](#)]

27. Leal-Junior, A.; Theodosiou, A.; Díaz, C.; Marques, C.; Pontes, M.J.; Kalli, K.; Frizzera-Neto, A. Fiber Bragg Gratings in CYTOP Fibers Embedded in a 3D-Printed Flexible Support for Assessment of Human-Robot Interaction Forces. *Materials* **2018**, *11*, 2305. [[CrossRef](#)]
28. Wang, S.; Zhang, B. Differential Soft Sensor-Based Measurement of Interactive Force and Assistive Torque for a Robotic Hip Exoskeleton. *Sensors* **2021**, *21*, 6545. [[CrossRef](#)]
29. Wilkening, A.; Puleva, N.; Ivlev, O. Estimation of Physical Human-Robot Interaction Using Cost-Effective Pneumatic Padding. *Robotics* **2016**, *5*, 17. [[CrossRef](#)]
30. Bessler, J.; Schaake, L.; Kelder, R.; Buurke, J.H.; Prange-Iasonder, G.B. Prototype Measuring Device for Assessing Interaction Forces between Human Limbs and Rehabilitation Robots—A Proof of Concept Study. In Proceedings of the 2019 IEEE 16th International Conference on Rehabilitation Robotics (ICORR), Toronto, ON, Canada, 24–28 June 2019; pp. 1109–1114.
31. Kim, T.; Jeong, M.; Kong, K. Bio-Inspired Knee Joint of a Lower-Limb Exoskeleton for Misalignment Reduction. *IEEE/ASME Trans. Mechatron.* **2021**, *4435*, 1–10. [[CrossRef](#)]
32. Langlois, K.; Roels, E.; Van De Velde, G.; Espadinha, C.; Van Vlerken, C.; Verstraten, T.; Vanderborght, B.; Lefeber, D. Integration of 3d Printed Flexible Pressure Sensors into Physical Interfaces for Wearable Robots. *Sensors* **2021**, *21*, 2157. [[CrossRef](#)]
33. Islam, M.R.U.; Bai, S. Payload Estimation Using Force Myography Sensors for Control of Upper-Body Exoskeleton in Load Carrying Assistance. *Model. Identif. Control* **2019**, *40*, 189–198. [[CrossRef](#)]
34. Long, Y.; Du, Z.J.; Chen, C.F.; Wang, W.D.; Dong, W. Development of a Lower Extremity Wearable Exoskeleton with Double Compact Elastic Module: Preliminary Experiments. *Mech. Sci.* **2017**, *8*, 249–258. [[CrossRef](#)]
35. Ghonasgi, K.; Yousaf, S.N.; Esmatloo, P.; Deshpande, A.D. A Modular Design for Distributed Measurement of Human–Robot Interaction Forces in Wearable Devices. *Sensors* **2021**, *21*, 1445. [[CrossRef](#)]
36. Leal-Junior, A.G.; Díaz, C.R.; Pontes, M.J.; Marques, C.; Frizzera, A. Polymer Optical Fiber-Embedded, 3D-Printed Instrumented Support for Microclimate and Human-Robot Interaction Forces Assessment. *Opt. Laser. Technol.* **2019**, *112*, 323–331. [[CrossRef](#)]
37. Mahdavian, M.; Toudeshki, A.G.; Yousefi-Koma, A. Design and Fabrication of a 3DoF Upper Limb Exoskeleton. In Proceedings of the 2015 3rd RSI International Conference on Robotics and Mechatronics (ICROM), Tehran, Iran, 7–9 October 2015; pp. 342–346. [[CrossRef](#)]
38. Huang, J.; Huo, W.; Xu, W.; Mohammed, S.; Amirat, Y. Control of Upper-Limb Power-Assist Exoskeleton Using a Human-Robot Interface Based on Motion Intention Recognition. *IEEE Trans. Autom. Sci. Eng.* **2015**, *12*, 1257–1270. [[CrossRef](#)]
39. Del-Ama, A.J.; Moreno, J.C.; Gil-Agudo, Á.; de-los-Reyes, A.; Pons, J.L. Online Assessment of Human-Robot Interaction for Hybrid Control of Walking. *Sensors* **2012**, *12*, 215–225. [[CrossRef](#)]
40. Beil, J.; Ehrenberger, I.; Scherer, C.; Mandery, C.; Asfour, T. Human Motion Classification Based on Multi-Modal Sensor Data for Lower Limb Exoskeletons. In Proceedings of the 2018 IEEE/RSJ International Conference on Intelligent Robots and Systems (IROS), Madrid, Spain, 1–5 October 2018; pp. 5431–5436. [[CrossRef](#)]
41. Lee, H.D.; Lee, B.K.; Kim, W.S.; Han, J.S.; Shin, K.S.; Han, C.S. Human-Robot Cooperation Control Based on a Dynamic Model of an Upper Limb Exoskeleton for Human Power Amplification. *Mechatronics* **2014**, *24*, 168–176. [[CrossRef](#)]
42. Levesque, L.; Pardoel, S.; Doumit, M. Experimental Comfort Assessment of an Active Exoskeleton Interface. In Proceedings of the 2017 IEEE International Symposium on Robotics and Intelligent Sensors (IRIS), Ottawa, ON, Canada, 5–7 October 2017.
43. Christensen, S.; Bai, S. Kinematic Analysis and Design of a Novel Shoulder Exoskeleton Using a Double Parallelogram Linkage. *J. Mech. Robot.* **2018**, *10*, 041008. [[CrossRef](#)]
44. Li, J.; Zuo, S.; Xu, C.; Zhang, L.; Dong, M.; Tao, C.; Ji, R. Influence of a Compatible Design on Physical Human-Robot Interaction Force: A Case Study of a Self-Adapting Lower-Limb Exoskeleton Mechanism. *J. Intell. Robot Syst. Theory Appl.* **2020**, *98*, 525–538. [[CrossRef](#)]
45. Schiele, A.; van der Helm, F.C.T. Influence of Attachment Pressure and Kinematic Configuration on PHRI with Wearable Robots. *Appl. Bionics Biomech.* **2009**, *6*, 157–173. [[CrossRef](#)]
46. Akiyama, Y.; Yamada, Y.; Ito, K.; Oda, S.; Okamoto, S.; Hara, S. Test Method for Contact Safety Assessment of a Wearable Robot Analysis of Load Caused by a Misalignment of the Knee Joint. In Proceedings of the 2012 IEEE RO-MAN: The 21st IEEE International Symposium on Robot and Human Interactive Communication, Paris, France, 9–13 September 2012; pp. 539–544. [[CrossRef](#)]
47. Bartenbach, V.; Wyss, D.; Seuret, D.; Riener, R. A Lower Limb Exoskeleton Research Platform to Investigate Human-Robot Interaction. In Proceedings of the 2015 IEEE International Conference on Rehabilitation Robotics (ICORR), Singapore, 11–14 August 2015; pp. 600–605. [[CrossRef](#)]
48. Amigo, L.E.; Fernandez, Q.; Giralt, X.; Casals, A.; Amat, J. Study of Patient-Orthosis Interaction Forces in Rehabilitation Therapies. In Proceedings of the 2012 4th IEEE RAS & EMBS International Conference on Biomedical Robotics and Biomechanics (BioRob), Rome, Italy, 24–27 June 2012; pp. 1098–1103. [[CrossRef](#)]
49. Long, Y.; Du, Z.; Chen, C.; Wang, W.; He, L.; Mao, X.; Xu, G.; Zhao, G.; Li, X.; Dong, W. Development and Analysis of an Electrically Actuated Lower Extremity Assistive Exoskeleton. *J. Bionic. Eng.* **2017**, *14*, 272–283. [[CrossRef](#)]
50. Masud, N.; Senkic, D.; Smith, C.; Isaksson, M. Modeling and Control of a 4-ADOF Upper-Body Exoskeleton with Mechanically Decoupled 3-D Compliant Arm-Supports for Improved-PHRI. *Mechatronics* **2021**, *73*, 102406. [[CrossRef](#)]
51. Tran, H.T.; Tan, L.N.; Han, S.H. Model-Learning-Based Partitioned Control of a Human-Powered Augmentation Lower Exoskeleton. *J. Electr. Eng. Technol.* **2022**, *17*, 533–550. [[CrossRef](#)]

52. Yousaf, S.N.; Esmatloo, P.; Ghonasgi, K.; Deshpande, A.D. A Method for the Analysis of Physical Human-Robot Interaction. In Proceedings of the 2021 IEEE/ASME International Conference on Advanced Intelligent Mechatronics (AIM), Delft, The Netherlands, 12–16 July 2021; pp. 1249–1254. [[CrossRef](#)]
53. Zannotto, D.; Akiyama, Y.; Stegall, P.; Agrawal, S.K. Knee Joint Misalignment in Exoskeletons for the Lower Extremities: Effects on User's Gait. *IEEE Trans. Robot* **2015**, *31*, 978–987. [[CrossRef](#)]
54. Lobo-Prat, J.; Kooren, P.N.; Janssen, M.M.H.P.; Keemink, A.Q.L.; Veltink, P.H.; Stienen, A.H.A.; Koopman, B.F.J.M. Implementation of EMG-and Force-Based Control Interfaces in Active Elbow Supports for Men with Duchenne Muscular Dystrophy: A Feasibility Study. *IEEE Trans. Neural Syst. Rehabil. Eng.* **2016**, *24*, 1179–1190. [[CrossRef](#)]
55. Wang, Y.; Qiu, J.; Cheng, H.; Zheng, X. Analysis of Human–Exoskeleton System Interaction for Ergonomic Design. *Hum. Factors* **2020**. [[CrossRef](#)]
56. Wan, X.; Liu, Y.; Akiyama, Y.; Yamada, Y. Monitoring Contact Behavior during Assisted Walking with a Lower Limb Exoskeleton. *IEEE Trans. Neural. Syst. Rehabil. Eng.* **2020**, *28*, 869–877. [[CrossRef](#)]
57. Kim, J.H.; Han, J.W.; Kim, D.Y.; Baek, Y.S. Design of a Walking Assistance Lower Limb Exoskeleton for Paraplegic Patients and Hardware Validation Using CoP. *Int. J. Adv. Robot Syst.* **2013**, *10*. [[CrossRef](#)]
58. Fan, Y.; Yin, Y. Active and Progressive Exoskeleton Rehabilitation Using Multisource Information Fusion from EMG and Force-Position EPP. *IEEE Trans. Biomed. Eng.* **2013**, *60*, 3314–3321. [[CrossRef](#)]
59. Rathore, A.; Wilcox, M.; Ramirez, D.Z.M.; Loureiro, R.; Carlson, T. Quantifying the Human-Robot Interaction Forces between a Lower Limb Exoskeleton and Healthy Users. In Proceedings of the 2016 38th Annual International Conference of the IEEE Engineering in Medicine and Biology Society (EMBC), Orlando, FL, USA, 16–20 August 2016; pp. 586–589. [[CrossRef](#)]
60. Wilcox, M.; Rathore, A.; Ramirez, D.Z.M.; Loureiro, R.C.V.; Carlson, T. Muscular Activity and Physical Interaction Forces during Lower Limb Exoskeleton Use. *Healthc. Technol. Lett.* **2016**, *3*, 273–279. [[CrossRef](#)]
61. Gcorgarakis, A.M.; Stampfli, R.; Wolf, P.; Riener, R.; Duarc, J.E. A Method for Quantifying Interaction Forces in Wearable Robots. In Proceedings of the 2018 7th IEEE International Conference on Biomedical Robotics and Biomechatronics (Biorob), Enschede, The Netherlands, 26–29 August 2018; pp. 789–794. [[CrossRef](#)]
62. Tran, H.T.; Cheng, H.; Lin, X.C.; Duong, M.K.; Huang, R. The Relationship between Physical Human–Exoskeleton Interaction and Dynamic Factors: Using a Learning Approach for Control Applications. *Sci. China Inf. Sci.* **2014**, *57*, 1–13. [[CrossRef](#)]
63. Long, Y.; Du, Z.J.; Wang, W.D.; He, L.; Mao, X.W.; Dong, W. Physical Human-Robot Interaction Estimation Based Control Scheme for a Hydraulically Actuated Exoskeleton Designed for Power Amplification. *Front. Inf. Technol. Electron. Eng.* **2018**, *19*, 1076–1085. [[CrossRef](#)]
64. Akiyama, Y.; Yamada, Y.; Okamoto, S. Interaction Forces beneath Cuffs of Physical Assistant Robots and Their Motion-Based Estimation. *Adv. Robot* **2015**, *29*, 1315–1329. [[CrossRef](#)]
65. Mouzo, F.; Michaud, F.; Lugris, U.; Cuadrado, J. Leg-Orthosis Contact Force Estimation from Gait Analysis. *Mech. Mach. Theory* **2020**, *148*, 103800. [[CrossRef](#)]
66. Quinlivan, B.; Asbeck, A.; Wagner, D.; Ranzani, T.; Russo, S.; Walsh, C. Force Transfer Characterization of a Soft Exosuit for Gait Assistance. In Proceedings of the International Design Engineering Technical Conferences and Computers and Information in Engineering Conference (ASME 2015), Boston, MA, USA, 2–5 August 2015; pp. 1–8. [[CrossRef](#)]
67. Xiloyannis, M.; Chiaradia, D.; Frisoli, A.; Masia, L. *Characterisation of Pressure Distribution at the Interface of a Soft Exosuit: Towards a More Comfortable Wear*; Springer: Berlin/Heidelberg, Germany, 2019; Volume 22, ISBN 9783030018870.
68. Huysamen, K.; de Looze, M.; Bosch, T.; Ortiz, J.; Toxiri, S.; O'Sullivan, L.W. Assessment of an Active Industrial Exoskeleton to Aid Dynamic Lifting and Lowering Manual Handling Tasks. *Appl. Ergon.* **2018**, *68*, 125–131. [[CrossRef](#)]
69. Akiyama, Y.; Okamoto, S.; Yamada, Y.; Ishiguro, K. Measurement of Contact Behavior Including Slippage of Cuff When Using Wearable Physical Assistant Robot. *IEEE Trans. Neural. Syst. Rehabil. Eng.* **2016**, *24*, 784–793. [[CrossRef](#)]
70. Awad, L.N.; Esquenazi, A.; Francisco, G.E.; Nolan, K.J.; Jayaraman, A. The ReWalk ReStore™ Soft Robotic Exosuit: A Multi-Site Clinical Trial of the Safety, Reliability, and Feasibility of Exosuit-Augmented Post-Stroke Gait Rehabilitation. *J. Neuroeng. Rehabil.* **2020**, *17*, 80. [[CrossRef](#)]
71. Hart, S.G.; Staveland, L.E. Development of NASA-TLX (Task Load Index): Results of Empirical and Theoretical Research. *Adv. Psychol.* **1988**, *52*, 139–183. [[CrossRef](#)]
72. Borg, G.A.V. Psychophysical Bases of Perceived Exertion. *Med. Sci. Sports Exerc.* **1982**, *14*, 377–381. [[CrossRef](#)]
73. World Union of Wound Healing Societies (WUWHS). *Role of Dressings in Pressure Ulcer Prevention: A Consensus Document*; World Union of Wound Healing Societies: Abu Dhabi, United Arab Emirates, 2016. [[CrossRef](#)]
74. Langlois, K.; Moltedo, M.; Bacek, T.; Rodriguez-Guerrero, C.; Vanderborcht, B.; Lefeber, D. Design and Development of Customized Physical Interfaces to Reduce Relative Motion between the User and a Powered Ankle Foot Exoskeleton. In Proceedings of the 2018 7th IEEE International Conference on Biomedical Robotics and Biomechatronics (Biorob), Enschede, The Netherlands, 26–29 August 2018; pp. 1083–1088. [[CrossRef](#)]
75. Norm, D. *ISO TR 23482-1; Safety-Related Test Methods for ISO 13482*. ISO: Geneva, Switzerland, 2008; Volume 2019, ISBN 9362178001.
76. Kermavnar, T.; Power, V.; De Eyto, A.; O'Sullivan, L.W. Computerized Cuff Pressure Algometry as Guidance for Circumferential Tissue Compression for Wearable Soft Robotic Applications: A Systematic Review. *Soft Robot* **2018**, *5*, 1–16. [[CrossRef](#)] [[PubMed](#)]

77. Lemming, D.; Graven-Nielsen, T.; Sørensen, J.; Arendt-Nielsen, L.; Gerdle, B. Widespread Pain Hypersensitivity and Facilitated Temporal Summation of Deep Tissue Pain in Whiplash Associated Disorder: An Explorative Study of Women. *J. Rehabil. Med.* **2012**, *44*, 648–657. [[CrossRef](#)] [[PubMed](#)]
78. Hven, L.; Frost, P.; Bonde, J.P.E. Evaluation of Pressure Pain Threshold as a Measure of Perceived Stress and High Job Strain. *PLoS ONE* **2017**, *12*, e0167257. [[CrossRef](#)] [[PubMed](#)]
79. Lacourt, T.E.; Houtveen, J.H.; van Doornen, L.J.P. Experimental Pressure-Pain Assessments: Test-Retest Reliability, Convergence and Dimensionality. *Scand. J. Pain.* **2012**, *3*, 31–37. [[CrossRef](#)] [[PubMed](#)]
80. Mikkelsen, M.; Latikka, P.; Kautiainen, H.; Isomeri, R.; Isomäki, H. Muscle and Bone Pressure Pain Threshold and Pain Tolerance in Fibromyalgia Patients and Controls. *Arch. Phys. Med. Rehabil.* **1992**, *73*, 814–818. [[CrossRef](#)]
81. Kermavnar, T.; O'Sullivan, K.J.; Casey, V.; de Eyto, A.; O'Sullivan, L.W. Circumferential Tissue Compression at the Lower Limb during Walking, and Its Effect on Discomfort, Pain and Tissue Oxygenation: Application to Soft Exoskeleton Design. *Appl. Ergon.* **2020**, *86*, 103093. [[CrossRef](#)]
82. Hobson, D.A. Comparative Effects of Posture on Pressure and Shear at the Body-Seat Interface. *J. Rehabil. Res. Dev.* **1992**, *29*, 21–31. [[CrossRef](#)]
83. Lachenbruch, C.; Tzen, Y.; Brienza, D.M.; Karg, P.E.; Lachenbruch, P.A. The Relative Contributions of Interface Pressure, Shear Stress, and Temperature on Tissue Ischemia: A Cross-Sectional Pilot Study. *Ostomy Wound Manag.* **2013**, *59*, 25–34.
84. Goossens, R.H.M.; Snijders, C.J.; Holscher, T.G.; Heerens, W.C.; Holman, A.E. Shear Stress Measured on Beds and Wheelchairs. *Scand. J. Rehabil. Med.* **1997**, *29*, 131–136.
85. Polliack, A.A.; Scheinberg, S. A New Technology for Reducing Shear and Friction Forces on the Skin: Implications for Blister Care in the Wilderness Setting. *Wilderness Environ. Med.* **2006**, *17*, 109–119. [[CrossRef](#)]
86. Goossens, R.H.M.; Zegers, R.; van Dijke, G.A.H.; Snijders, C.J. Influence of Shear on Skin Oxygen Tension. *Clin. Physiol.* **1994**, *14*, 111–118. [[CrossRef](#)] [[PubMed](#)]
87. Chimata, G.P.; Schwartz, C.J. Investigation of the Effect of the Normal Load on the Incidence of Friction Blisters in a Skin-Simulant Model. *Proc. Inst. Mech. Eng. Part J J. Eng. Tribol.* **2015**, *229*, 266–272. [[CrossRef](#)]
88. He, Y.; Eguren, D.; Luu, T.P.; Contreras-Vidal, J.L. Risk and Adverse Events Related to Lower-Limb Exoskeletons. In Proceedings of the 2017 International Symposium on Wearable Robotics and Rehabilitation (WeRob), Houston, TX, USA, 5–8 November 2017; pp. 1–2. [[CrossRef](#)]
89. Schick, J.; Glaser, M.; Kennel, R. Risk Assessment and Mitigation Strategies for Active Lower Limb Exoskeletons. In Proceedings of the 2020 Annual Reliability and Maintainability Symposium (RAMS), Palm Springs, CA, USA, 27–30 January 2020. [[CrossRef](#)]
90. He, Y.; Eguren, D.; Luu, T.P.; Contreras-Vidal, J.L. Risk Management and Regulations for Lower Limb Medical Exoskeletons: A Review. *Med. Devices Evid. Res.* **2017**, *10*, 89–107. [[CrossRef](#)] [[PubMed](#)]
91. Reswick, J.B.; Rogers, J.E. Experience at Rancho Los Amigos Hospital with Devices and Techniques to Prevent Pressure Sores. In *Bed Sore Biomechanics*; Springer: Berlin, Germany, 1976; Volume 2, pp. 301–310. [[CrossRef](#)]
92. Mao, X.; Yamada, Y.; Akiyama, Y.; Okamoto, S.; Yoshida, K. Safety Verification Method for Preventing Friction Blisters during Utilization of Physical Assistant Robots. *Adv. Robot* **2017**, *31*, 680–694. [[CrossRef](#)]
93. Mao, X.; Yamada, Y.; Akiyama, Y.; Okamoto, S.; Yoshida, K. Development of a Novel Test Method for Skin Safety Verification of Physical Assistant Robots. In Proceedings of the 2015 IEEE International Conference on Rehabilitation Robotics (ICORR), Singapore, 11–14 August 2015; pp. 319–324. [[CrossRef](#)]
94. Kermavnar, T.; O'Sullivan, K.J.; de Eyto, A.; O'Sullivan, L.W. Relationship Between Interface Pressures and Pneumatic Cuff Inflation Pressure at Different Assessment Sites of the Lower Limb to Aid Soft Exoskeleton Design. *Hum. Factors* **2020**, *63*, 1061–1075. [[CrossRef](#)]